

## Peak Intensity Measurements in the Early Days of AES

J.T. Grant

*Research Institute, University of Dayton, 300 College Park, Dayton OH 45469-0168, USA*

*j.grant@ieee.org*

*Received 8 January 2002; Accepted 17 January 2003*

In the early days of Auger electron spectroscopy (AES), lock-in amplifiers were used to measure the first derivative of the electron energy distribution,  $N(E)$ , and Auger intensities were determined using the peak-to-peak heights of Auger features. Such measures of intensity were accurate only if the Auger lineshape of the measured peak was identical to that from a reference spectrum. This was rarely the case, and attempts were made by many researchers to determine better values for Auger intensities. These studies were made in the 1970's, and were made before the introduction of dedicated computers for data acquisition and processing. This paper reviews many of the early problems with quantitative analysis using peak-to-peak heights, and some of the approaches used to overcome them.

### INTRODUCTION

Although Jim Lander recognized in 1953 that certain peaks in secondary electron energy distributions were from Auger electrons, and they would be useful for studying the composition of solid surfaces, the difficulty in detecting them due to their superposition on the large, slowly varying background of secondary and backscattered electrons detracted from their usefulness at that time[1]. It was not until 1967, when Larry Harris showed that electronic differentiation enhanced the Auger spectral features, that AES became a practical tool for surface analysis[2]. Although he initially used differentiation with a simple RC circuit, it was the lock-in amplifier that made differentiation feasible (independent of sweep rate and sweep direction; of course, lock-in amplifiers also have a time constant, but that only affects the spectra when the sweep rate is fast in relation to the time constant). Roland Weber and Bill Peria used this information to obtain derivative Auger spectra in a LEED (low energy electron diffraction) system with a lock-in amplifier[3, 4]. Numerous LEED systems were in operation around the world in the late 1960's, and many of these were modified to conduct Auger electron spectroscopy measurements on materials. This is when Auger electron spectroscopy became a widely used technique for surface analysis.

Surface composition was obtained by identifying the Auger peaks at various kinetic energies, and the concen-

trations of the elements were obtained from the peak intensities. Although the area under an Auger peak corresponds to the Auger current, Auger peak-to-peak heights were used as a measure of the Auger current. This is reliable only if the measured Auger lineshape is identical to that from a reference spectrum for that element. The Auger lineshape can be affected by the modulation amplitude used on the energy analyzer for obtaining the derivative spectrum[5, 6], and by changes in chemistry of the element detected[7, 8]. Several approaches were used to correct for such problems, and it is some of these approaches that are reviewed here.

JEOL introduced their first commercial Auger instrument in 1974, the JAMP-3. The author was at the 6th International Vacuum Congress and 2nd International Conference on Solid Surfaces in Kyoto, Japan, 25-29 March, 1974 when JEOL demonstrated their first commercial instrument. Four years later, they introduced the JAMP-10, in which one could also modulate the intensity of the incident electron beam (beam brightness modulation) to obtain the so-called "direct" Auger spectrum with a lock-in amplifier, as well as modulate the analyzer energy to obtain the derivative spectrum. The beam brightness modulation method was developed by Mogami and Sekine[9]. Sekine was also instrumental in publishing the *JEOL Handbook of Auger Electron Spectroscopy*, which was the first to show the direct spectra of the elements[10].

### PEAK INTENSITY MEASUREMENTS

In the 1970's, there were many approaches to improve peak intensity measurements for quantitative Auger analysis. The approaches given here cover (i) the instrument response formalism, (ii) dynamic background subtraction, using digital and analog integration, and (iii) tailored modulation techniques. All these methods were useful in obtaining better measures of Auger intensities in that they could correct for lineshape changes due to analyzer modulation or changes in chemistry. Even though most Auger spectra today are measured in the direct form and modulation effects have been eliminated, derivatives of spectra are usually taken in a computer and the peak-to-peak heights are then used for quantitative analysis. This is an accurate measure of intensity only if the derivative lineshapes are identical to reference spectra. Therefore some of these old approaches can still be used to improve quantification, although these problems can be minimized if the Auger peaks are artificially broadened when the derivatives are taken[11].

#### Instrument Response Formalism

The effects of distortion due to modulation of the analyzer potential were calculated by Hugh Bishop and John Rivière[5], and by Norm Taylor[6], for both deflection type analyzers and retarding field analyzers. These studies assumed that the Auger lineshape was Gaussian. For deflection type analyzers, it was found that the peak-to-peak height increased linearly with modulation amplitude up to a certain point, then passed through a maximum, after which it decreased with further increases in modulation. For the retarding field analyzer, the peak-to-peak height increased as the square of the modulation amplitude up to a certain point, and then approached a constant value independent of the modulation amplitude.

The behavior of the peak-to-peak height of a derivative Auger peak depends on the actual shape of an Auger peak. The above analysis applies only to Gaussian peaks, and the Taylor series analysis used applies only where the modulation amplitude is small with respect to the widths of the features. Jack Houston, using an instrument response formalism, showed that the double integral of a measured derivative spectrum over its entire structure could be simply and exactly related to the area measured in the absence of distortion due to modulation[12]. He also showed that this did not depend on the shape of the Auger peak, and that it was valid for all modulation amplitudes.

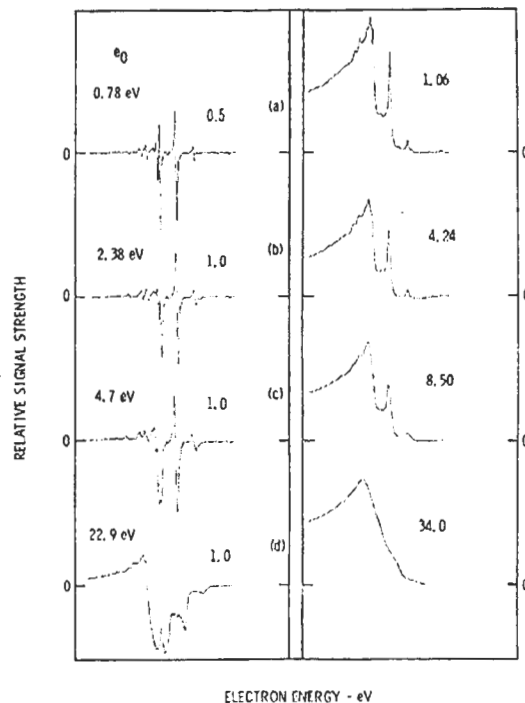


Fig. 1. The left hand panel shows the derivative LMM Auger spectra of Ti for different modulations. The right hand panel shows the corresponding results after one integration of the derivative data. The data have been attenuated by the factors shown.

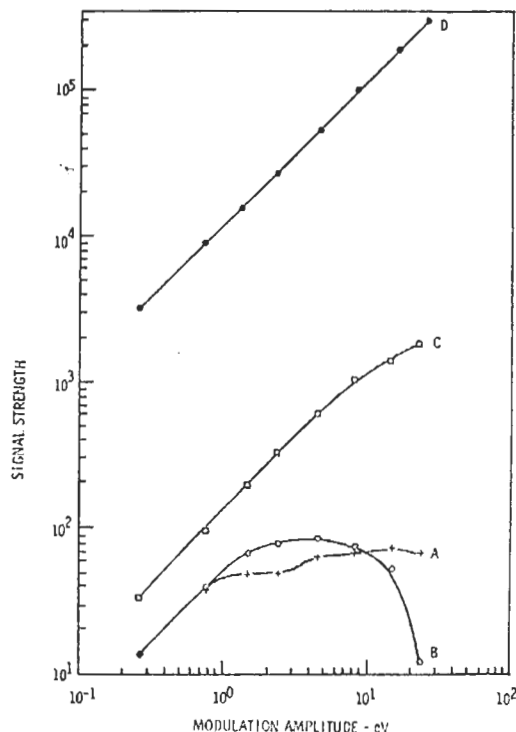


Fig. 2. Variations of Auger signal strengths with modulation amplitude for a deflection type analyzer. A and B are for Ti LMM peak-to-peak heights, C is overall peak height in E.N(E), and D are the area values.

This was verified experimentally for both deflection type analyzers[13] and retarding field analyzers[14]. An example for a deflection type analyzer is shown in Figs. 1 and 2. The left-hand box in Fig. 1 shows derivative Auger spectra from Ti for various modulation amplitudes (including the spectrometer factor to give equivalent energies). Note the severe peak distortions at higher modulations. The peak-to-peak heights of the two major features (just below and just above 400 eV) are shown as curves A and B in Fig. 2. The intermediate results obtained after one integration over the entire Auger structure are shown as peak heights in curve C of Fig. 2, and the corresponding spectral results are shown in the right-hand box of Fig. 1. The results of double integration of the derivative spectra are shown in curve D, where it can be seen that the intensity is now exactly linear with modulation amplitude for all modulations, even when the spectra are severely distorted. This also means that spectra from different elements in survey spectra can also be exactly compared, no matter what their individual lineshapes are, or what modulation amplitudes were used. This was also verified experimentally[15].

For retarding field analyzers, the double integral of derivative Auger spectra increases as the square of the modulation amplitude, and this was verified experimentally over a wide range of modulations[14]. The corresponding results for Ti obtained in a retarding field analyzer are shown in Fig.3. Note that curve D now increases with the square of the modulation amplitude. It was also

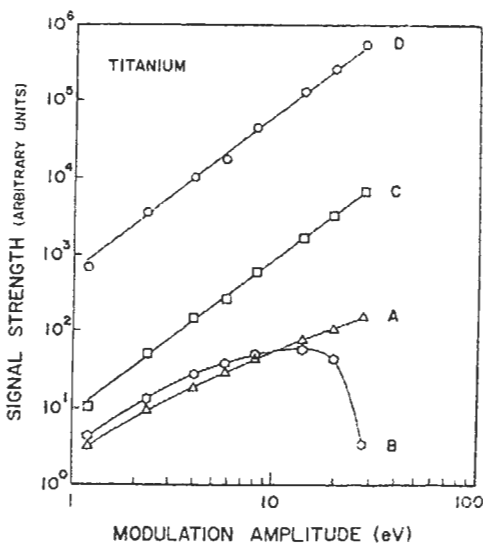


Fig. 3. Variations of Auger signal strengths with modulation amplitude for a retarding field analyzer. A and B are for Ti LMM peak-to-peak heights, C is overall peak height in N(E), and D are the area values.

shown that integration corrects for small misalignments in sample position in retarding field analyzers[14].

### Dynamic Background Subtraction

Dynamic Background Subtraction (DBS) involves multiple differentiations followed by multiple integrations of some experimental variable. The theoretical basis for this operation was examined by Jack Houston, who showed that when sufficient derivatives are taken to remove the background, the Auger features may be recovered by multiple integrations[16].

DBS has been used in many applications for AES, and was also found very useful for removing backgrounds in appearance potential spectroscopy[17]. In AES, it has been used in both deflector type analyzers and retarding field analyzers. Multiple derivatives could be taken until the background was removed with a lock-in amplifier with suitable harmonic detection[18], while the integration could be done digitally in a signal averager (at the time), or by using analog methods. At each stage of integration, the data on the high kinetic energy side of the Auger peaks must be set to zero.

One problem with this approach for quantitative analysis involves the energy range of integration, as the slowly varying loss structure associated with Auger peaks remains, and the integrals do not converge. However, by establishing energy ranges for integration, excellent quantitative comparisons are possible for the same element in different chemical forms[19, 20], and between different elements, for example carbon and oxygen[21, 22].

### Lock-in Amplifier and Digital Integration

An example of the application of DBS to determine changes in carbon and oxygen concentrations is shown in Figs. 4 and 5, where molecularly adsorbed CO on clean Ni (110) has undergone electron beam damage. The derivative Auger spectra, Fig. 4, have removed the background from the spectra, but the changes in lineshapes of both the carbon and oxygen peaks prohibit the use of peak-to-peak heights for following changes in concentrations for each element or between them.

Figure 5 shows the corresponding spectra after one of the integration steps. Note also the improvement in signal-to-noise. A second integration measures the area under the peaks, and allows comparisons to be made in carbon or oxygen concentrations as a function of electron beam exposure. The carbon and oxygen concentrations were

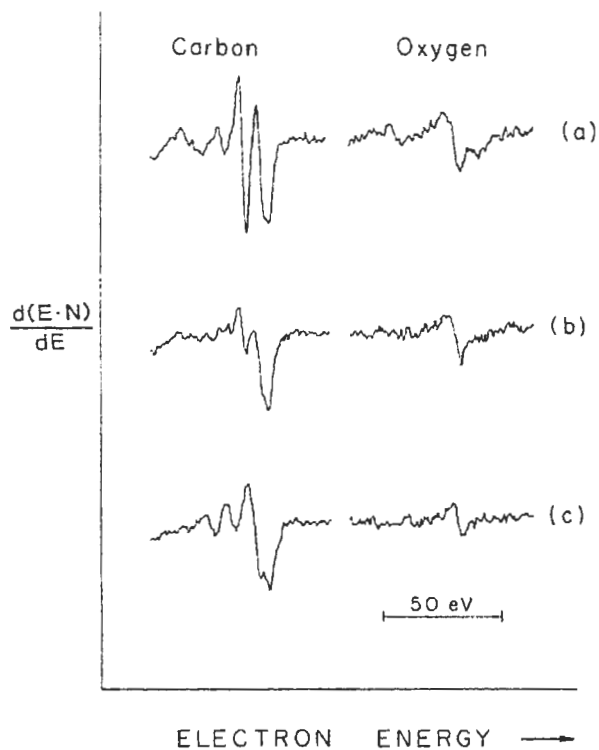


Fig. 4. Derivative C and O Auger spectra: (a) after exposure of clean Ni (110) to CO; (b) after exposure to a 1.5  $\mu$ A, 1.5 keV electron beam for 10 min.; and (c) after exposure to the beam for 40 min.

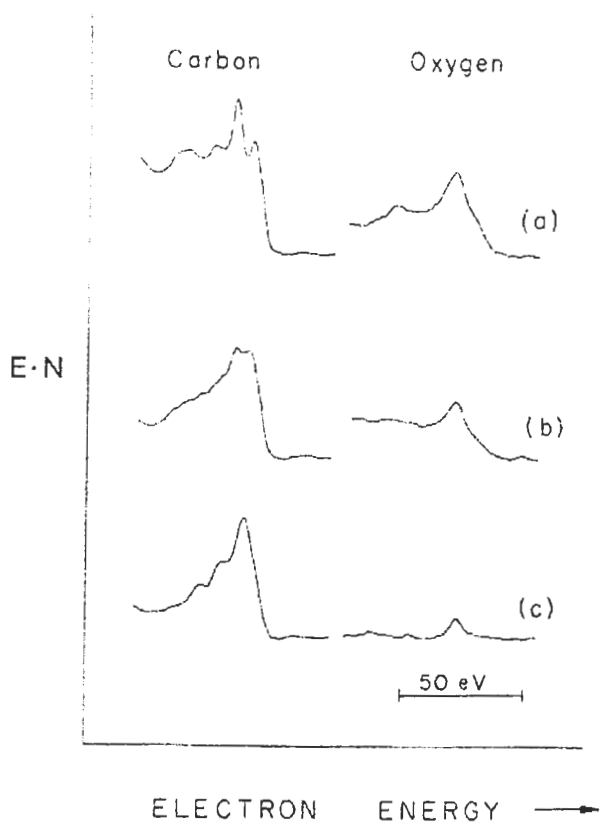


Fig. 5. The C and O Auger data from Fig. 4 after one integration.

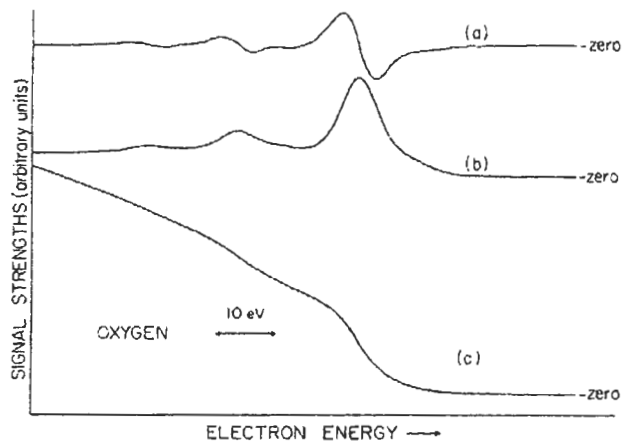


Fig. 6. O Auger spectra for CO on Mo (110): (a) derivative spectrum from lock-in amplifier; (b) spectrum obtained after one analog integration of lock-in output; and (c) result after double analog integration of lock-in output.

found to decrease by 10 and 35 % respectively after 10 min beam exposure, and by 30 and 90 % after 40 min beam exposure[22].

#### Lock-in Amplifier and Analogue Integration

Analog integration has also been used to integrate the signal from the lock-in amplifier[21]. An example of this is shown in Fig. 6, where part (a) shows the derivative Auger spectrum from oxygen with the background set to zero, part (b) the output from one analog integration, and part (c) the output after double integration of the derivative signal. Therefore, part (c) shows the area under the Auger peak as a function of the integration range.

Analog integration was applied to measure the carbon to oxygen atomic ratio after CO was adsorbed on a clean Mo (110) surface[21]. The output from the lock-in amplifier is shown in Fig. 7. Double analog integration was carried out over an energy range of 44 eV, starting just on the high energy side of the carbon and oxygen Auger features. (It was shown that the range of integration has only a small effect, < 5 %, on relative intensities.) After appropriate corrections, the ratio of the carbon to oxygen was found to be  $1.09 \pm 0.05$  where the uncertainty is for the integration only, and not uncertainties in the correction terms[21].

The adsorption of CO on clean Ni (110) was also investigated with digital integration of the carbon and oxygen Auger peaks[22]. The derivative Auger spectrum after CO adsorption is shown in Fig. 8. Note that the carbon Auger lineshape is quite different from that obtained with

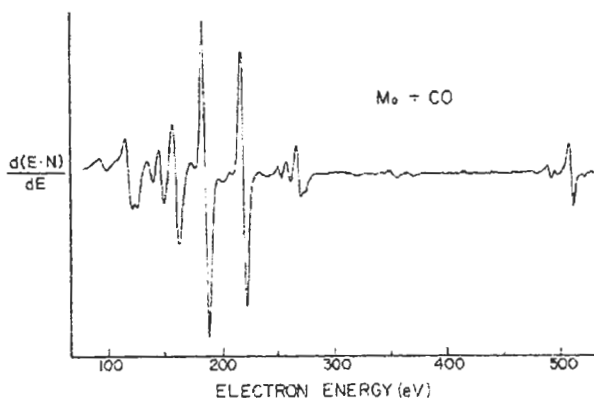


Fig. 7. Derivative Auger spectrum for CO on clean Mo (110)

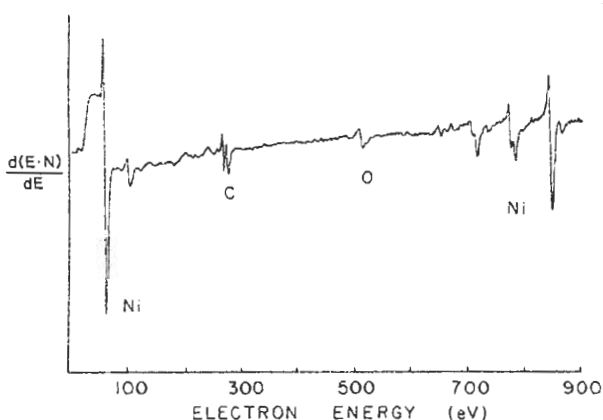


Fig. 8. Derivative Auger spectrum for CO on clean, ion bombarded Ni.

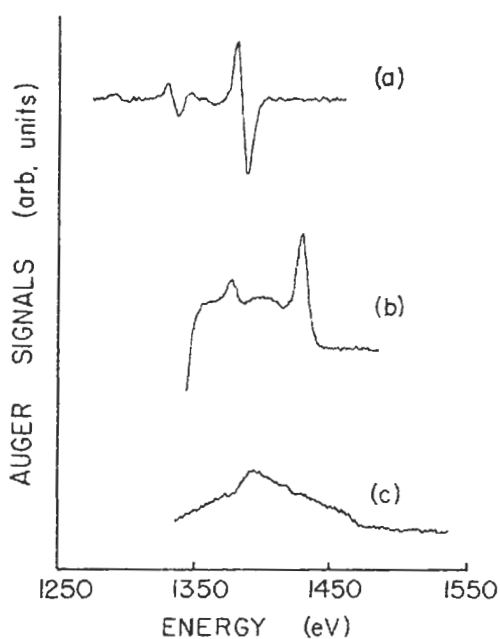


Fig. 9. Al KLL Auger signals from  $Al_2O_3$ : (a) derivative spectrum obtained with small square wave modulation; (b) the energy distribution obtained using TMT with a large square wave modulation; and (c) the dependence of Auger area value with the range of integration, obtained using TMT.

CO adsorption on Mo (110)[21]. CO is known to adsorb molecularly on Ni (110), bonding to the Ni via the carbon atom, and the carbon and oxygen lineshapes observed here are very similar to those obtained on other metals where similar molecular adsorption occurs[23].

Double digital integration of the carbon and oxygen Auger features in Fig. 8 over the same energy range of 44 eV used for analog integration with CO on Mo, gives a carbon to oxygen atomic ratio of 1.02, with an uncertainty of 20 % as determined over three adsorption runs[22].

DBS has been used in many other applications as well. One worth mentioning is the case of oxygen adsorption on ion bombarded Ni, where DBS shows that quantitative analysis using peak-to-peak heights can produce errors of a factor of two in measuring the oxygen Auger current due to subtle changes in the lineshape of its derivative Auger spectrum[20].

#### Tailored Modulation Techniques

With tailored modulation techniques (TMT), the modulation waveform is tailored to the instrument response function and the degree of background subtraction required, allowing areas under Auger peaks to be measured *directly* from the output of the lock-in amplifier[18]. A direct comparison of results obtained from DBS and TMT showed almost perfect proportionality between the results[24].

Examples of the output signals from the lock-in amplifier for the Al KLL Auger peaks, are shown in Fig. 9 for a deflection type analyzer[25]. The usual first derivative spectrum is shown in Fig. 9a, and was obtained with a small square wave modulation (5 eV peak-to-peak) on the analyzer. The electron energy distribution obtained directly from the lock-in amplifier is shown in Fig. 9b. Note the absence of background on the high energy side of the Auger spectrum. This distribution was obtained using a large square wave modulation (85 eV peak-to-peak) on the analyzer. With this modulation waveform, the measured electron energy distribution shifts to higher energy by half the modulation amplitude. This does not cause any problems in peak identification, since the shift is known exactly. The electron energy distributions are valid over energy ranges equal to the modulation energy used (here 85 eV) measured from the high energy threshold of each set of peaks. Beyond this range, inverted, complementary spectra appear, thereby limiting this technique to Auger spectra that are not too crowded.

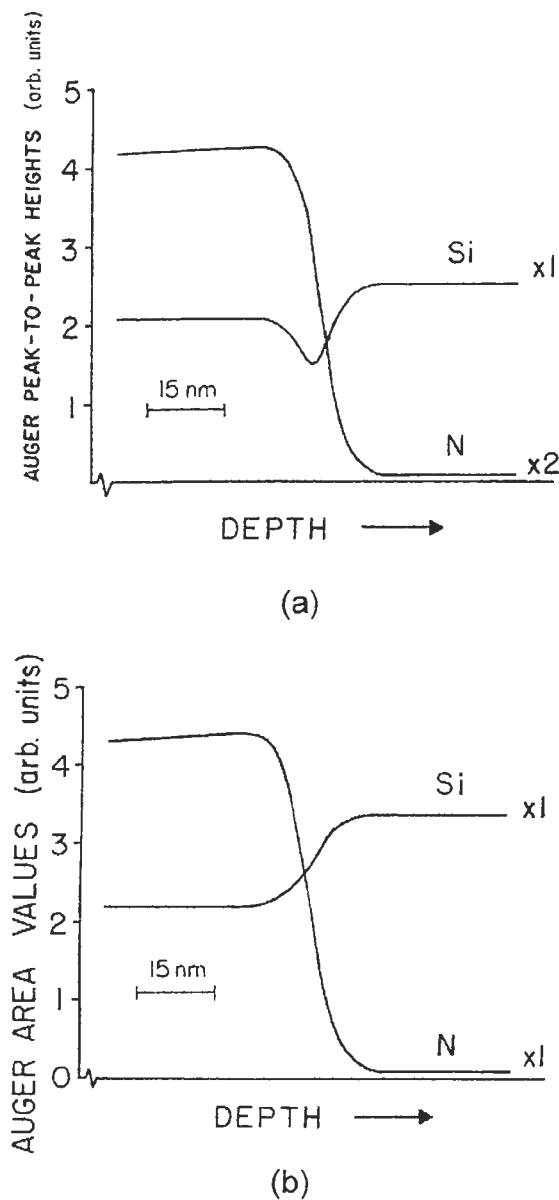


Fig. 10. Sputter depth profiles of  $\text{Si}_3\text{N}_4$  on Si showing Si and N signals obtained using: (a) peak-to-peak heights of the KLL transitions, and (b) Auger area values obtained using TMT.

The application of TMT to obtain Auger area values is shown in Fig. 9c. This result was obtained by modulating the analyzer with a waveform that was the sum of a square wave and a cosine wave, each having peak-to-peak amplitudes of 85 eV. The high energy threshold now appears 85 eV above the derivative spectrum, and this distribution now gives Auger area values as a function of the energy range of integration (here, up to 85 eV) from the high energy Auger threshold. After the maximum energy range is reached, the output from the lock-in amplifier decreases slowly. When coupled with an analog multiplexing system, such as was used for depth profiling at the time, it

was possible to measure Auger peak areas. This was accomplished by adjusting the multiplex channels to include such peaks in the output signal as well as the zero reference level above the high energy threshold of the Auger structure. The range of integration was then determined by the size of the modulation.

TMT was used in depth profiling to automatically correct for effects of Auger lineshape changes on depth profiles[25, 26]. An example of this is shown in Fig. 10 for sputter depth profiles of  $\text{Si}_3\text{N}_4$  on Si. When peak-to-peak heights in the derivative spectra are used to measure the silicon Auger intensity, an artifact occurs near the  $\text{Si}_3\text{N}_4$ /Si interface. This is shown in Fig. 10a, and is due to the chemical shift in the KLL Auger peak energies between  $\text{Si}_3\text{N}_4$  and Si, and not to a decrease in silicon concentration[25]. As the interface is approached, the Si  $\text{KL}_{2,3}\text{L}_{2,3}$  signal from  $\text{Si}_3\text{N}_4$  decreases while that from Si increases, but because there is a 5 eV difference in the Auger kinetic energy between these two silicon chemistries, the peak-to-peak height in the combined energy region will decrease at first.

A depth profile of the same film obtained using TMT is shown in Fig. 10b. Note that the artifact in the silicon profile has been removed, and the silicon signal increases as the interface is approached. In this example, the modulation amplitude was set so the integration of the Auger current was carried out over 35 eV. Similar results were obtained for  $\text{SiO}_2$  on Si[25], and  $\text{Al}_2\text{O}_3$  on Al[26].

## SUMMARY

I was deeply saddened to learn of the death of Dr. Sekine on 31 January 2002. In this paper, I have tried to give an historical perspective on some of the developments in processing Auger data in the 1970's, when I first met Dr. Sekine. These were exciting times.

## References

- [1] J. J. Lander, *Phys. Rev.* **91**, 1382 (1953).
- [2] L. A. Harris, *J. Appl. Phys.* **39**, 1419 (1968).
- [3] R. E. Weber and W. T. Peria, *J. Appl. Phys.* **38**, 4355 (1967).
- [4] L. A. Harris, *J. Vac. Sci. Technol.* **11**, 23 (1974).
- [5] H. E. Bishop and J. C. Rivière, *J. Appl. Phys.* **40**, 1740 (1969).
- [6] N. J. Taylor, *Rev. Sci. Instrum.* **40**, 792 (1969).
- [7] T. W. Haas and J. T. Grant, *Appl. Phys. Lett.* **16**, 172 (1970).

- [8] T. W. Haas, J. T. Grant and G. J. Dooley, *J. Appl. Phys.* **43**, 1853 (1972).
- [9] A. Mogami and T. Sekine, *Proceedings of 6th European Congress on Electron Microscopy*, Jerusalem, p. 422, TAL International, Israel (1976).
- [10] T. Sekine, Y. Nagasawa, M. Kudoh, Y. Sakai, A. S. Parkes, J. D. Geller, A. Mogami, and K. Hirata, *Handbook of Auger Electron Spectroscopy*, JEOL, Japan (1982).
- [11] M. P. Seah, *J. Electron Spectrosc. Relat. Phenom.* **100**, 55 (1999).
- [12] J. E. Houston, *Surf. Sci.* **38**, 283 (1973).
- [13] J. T. Grant, T. W. Haas and J. E. Houston, *Surf. Sci.* **42**, 1 (1974).
- [14] J. T. Grant and T. W. Haas, *Surf. Sci.* **44**, 617 (1974).
- [15] J. T. Grant, M. P. Hooker and T. W. Haas, *J. Colloid Interface Sci.* **55**, 370 (1976).
- [16] J. E. Houston, *Rev. Sci. Instrum.* **45**, 897 (1974).
- [17] J. T. Grant, T. W. Haas and J. E. Houston, *Japan. J. Appl. Phys., Suppl.2*, Pt.2, 811 (1974).
- [18] R. W. Springer and D. J. Pocker, *Rev. Sci. Instrum.* **48**, 74 (1977).
- [19] J. T. Grant, T. W. Haas and J. E. Houston, *Phys. Lett.* **45A**, 309 (1973).
- [20] M. P. Hooker, J. T. Grant and T. W. Haas, *J. Vac. Sci. Technol.* **13**, 296 (1976).
- [21] J. T. Grant, M. P. Hooker and T. W. Haas, *Surf. Sci.* **46**, 672 (1974).
- [22] M. P. Hooker and J. T. Grant, *Surf. Sci.* **55**, 741 (1976).
- [23] M. P. Hooker and J. T. Grant, *Surf. Sci.* **62**, 21 (1977).
- [24] R. W. Springer, D. J. Pocker and T. W. Haas, *Appl. Phys. Lett.* **27**, 368 (1975).
- [25] J. T. Grant, R. G. Wolfe, M. P. Hooker, R. W. Springer and T. W. Haas, *J. Vac. Sci. Technol.* **14**, 232 (1977).
- [26] J. T. Grant, M. P. Hooker, R. W. Springer and T. W. Haas, *Surf. Sci.* **60**, 1 (1976).